Air Energy and Risk Trajectory Optimisation

Alex Blakesley

March 3, 2023

This chapter describes the methodology for optimising a trajectory between an origin and destination whilst minimising both energy consumption and risk for a quad-copter UAV to aid in logistics planning and operations.

1 Minimum Energy Trajectory Optimisation Framework

This section describes the fundamentals of UAV minimum energy route optimisation of a quad-copter UAV. It will lay out the structures that are required to define the problem and will use dynamics, objective functions and constraints found throughout the literature to test the effectiveness of these models in a basic test case.

1.1 State, Control and Objective Function

The state space consists of a UAV's position and rotation, as well as its rate of change, i.e.

$$[x, y, z, \dot{x}, \dot{y}, \dot{z}, \phi, \theta, \psi, \dot{\phi}, \dot{\theta}, \dot{\psi}]^\top, \tag{1}$$

whilst control inputs are set to the angular velocity of the four motors

$$[\omega_1, \omega_2, \omega_3, \omega_4]^\top. \tag{2}$$

The objective function aims to reduce energy consumption, such that

$$\min_{\omega_i} \sum_{i=1}^{4} \int_{t_0}^{t_f} \omega_i^3 \, dt, \tag{3}$$

which acts as a proxy for energy minimisation as the greater the total value of ω across all four motors, the greater the power consumption of the UAV.

As mentioned previously, this objective function will also include the minimisation of risk, however this is currently planned as future work.

1.2 Equations of Motion

The dynamic formulation follows [1], but some of the equations have been improved to include the impact of drag on the dynamics as well as a factor to incentivise the drone to land, which is a crucial requirement and the reasoning of which is described in [2]. These are then combined with six further equations which add constraints on the problem by defining how the rate of change of a state variable is related to its symbolic counterpart, which gives the complete set of dynamic equations as follows:

$$m\ddot{x} = (\cos\phi \sin\theta \cos\psi + \sin\theta \sin\psi)T - D(\dot{x}), \tag{4}$$

$$m\ddot{y} = (\cos\phi \sin\theta \sin\psi - \sin\theta \cos\psi)T - D(\dot{y}), \tag{5}$$

$$m\ddot{z} = (\cos\phi \cos\theta)T - mg\lambda(x, y, z) - D(\dot{z}), \tag{6}$$

$$\dot{x} = \frac{dx}{dt}, \tag{7}$$

$$\dot{y} = \frac{dy}{dt}, \tag{8}$$

$$\dot{z} = \frac{dz}{dt}, \tag{9}$$

$$I_x\ddot{\phi} = (I_y - I_z)\dot{\theta}\dot{\psi} + (F_2 - F_4)l + J\dot{\theta}\bar{\omega} \tag{10}$$

$$I_y\ddot{\theta} = (I_z - I_x)\dot{\psi}\dot{\phi} + (F_3 - F_1)l - J\dot{\phi}\bar{\omega} \tag{11}$$

$$I_z\ddot{\psi} = (I_x - I_y)\dot{\phi}\dot{\theta} + (M_1 - M_2 + M_3 - M_4), \tag{12}$$

$$\dot{\phi} = \frac{d\phi}{dt}, \tag{13}$$

$$\dot{\theta} = \frac{d\theta}{dt}, \tag{14}$$

$$\dot{\psi} = \frac{d\psi}{dt}, \tag{15}$$

where $F_i = k_b(\omega_i^2)$, $M_i = k_\tau(\omega_i^2)$, $T = \sum_{i=1}^{4} F_i$, $k_b = C_T\rho Ar^2$ is the thrust factor, $k_\tau = C_Q\rho Ar^3$ is the drag factor, $\bar{\omega} = \omega_1 - \omega_2 + \omega_3 - \omega_4$, $J = J_m + J_l$ where the J_m denotes motor moments of inertia and $J_l = \frac{1}{4}n_B m_B(r-e)^2$ is load moment of inertia, D is the drag acting on the body of the UAV, λ is the landing incentivisation adjustment which is defined in [2] and all other parameters are given in table 1.

Table 1: Parameters and their values used to model the energy consumption and dynamics of a quadcopter UAV. The values are based on a DJI phantom 2 [3, 4] and were used in both test cases.

Panel A: Parameter values independent of drone			
Variable	Symbol	Value	Units
Air density	ρ	1.225	kg/m^3
Acceleration due to gravity	g	9.8066	m/s^2
Panel B: Static parameter values dependent on drone			
Number of rotor blades	n_B	4	-
Blade to motor hub offset	ϵ	4e-3	m
Mass of a blade	m_B	5.5e-3	kg
Radius of the propeller	r	0.12	m
Spinning area of one rotor	A	0.0507	m^2
Drone arm length	l	0.175	m
Mass of drone body	m	1.3	kg
Propeller thrust coefficient	C_T	4.8e-3	-
Propeller torque coefficient	C_Q	2.35e-4	-
Rotor moment of inertia	J_m	4.9e-6	kg m^2
X component of body inertia	I_x	0.081	kg m^2
Y component of body inertia	I_y	0.081	kg m^2
Z component of body inertia	I_z	0.142	kg m^2
Maximum angular velocity	ω_{max}	1000	rad/s
Panel C: Dynamic parameter values describing the drone			
Position in x, y, z	x, y, z	-	m
Velocity in x, y, z	$\dot{x}, \dot{y}, \dot{z}$	-	m/s
Acceleration in x, y, z	$\ddot{x}, \ddot{y}, \ddot{z}$	-	m/s^2
Drone roll, pitch, yaw	ϕ, θ, ψ	-	rad
Roll, pitch, yaw velocity	$\dot{\phi}, \dot{\theta}, \dot{\psi}$	-	rad/s
Roll, pitch, yaw acceleration	$\ddot{\phi}, \ddot{\theta}, \ddot{\psi}$	-	rad/s^2
Rotor angular velocity	ω_i	-	rad/s

1.3 Constraints

Instance constraints are a snapshot of the state vector given at a certain point in the time horizon. The most important of these are the initial and final instance constraints, which are defined at the start of the route, t_0,

$$[x_0, y_0, z_0, 0 \times 9]^\top, \tag{16}$$

and at its end, t_f,

$$[x_f, y_f, z_f, 0 \times 9]^\top. \tag{17}$$

Finally, the physical bounds are applied to the problem:

$$\begin{aligned} 0 \leq \omega_i \leq \omega_{max} \\ 0 \leq z \\ -\pi/10 \leq \phi \leq \pi/10 \\ -\pi/10 \leq \theta \leq \pi/10. \end{aligned} \tag{18}$$

The optimisation problem is discretised using the trapezoidal collocation method [5] into 500 nodes, and subsequently solved numerically using the interior point line search filter method as implemented in the IPOPT solver [6]. The acceptable convergence tolerance for the algorithm was set to 10^{-4}.

2 Minimum Energy and Risk Trajectory Optimisation Framework

This section describes the changes made to the formulation of the problem in order to effectively minimise both energy and risk, given a weighting factor, when generating a trajectory between two locations. Results are also given which show the effect of the weighting factor on the results.

2.1 Formulation

In order effectively minimise both energy and risk, a value for the risk at a spatial co-ordinate is required. The calculation of risk is done through the e-Drone RO module and will not be explored within this chapter. The risk is a function of the position and velocity of the UAV and can be included within the objective function when applied to a weighting factor and is given by:

$$\min_{\omega_i} \sum_{i=1}^{4} \int_{t_0}^{t_f} \omega_i^3 \, dt + \alpha R(x, y, z, \dot{x}, \dot{y}, \dot{z}), \tag{19}$$

where R is a function of ground risk.

2.2 Results

In order to show the effectiveness of the framework it is applied to a test case where the optimiser generates a trajectory from Southampton General Hospital to Hythe Hospital, both of which are in the Solent region of the UK.

The start location is $\tilde{\boldsymbol{x}}_0 = [50.933°, -1.434°, 0]^\top$ and destination is $\tilde{\boldsymbol{x}}_f = [50.859°, -1.403°, 0]^\top$, where $\tilde{\boldsymbol{x}}$ is the position vector given in [latitude, longitude, altitude] format, which is then converted to a UTM coordinate system [7] and then localised about the origin, so that $\boldsymbol{x}_0 = [0, 0, 0]^\top$ and $\boldsymbol{x}_f = [-2409.26, 8203.15, 0]^\top$. The maximum number of iterations was set to 5,000.

The experiment is run twice, once where $\alpha = 5 \times 10^8$ and once where $\alpha = 5 \times 10^9$, in order to compare a more energy optimal route to a more risk optimal route. The results are show in fig. 1, where is can be seen that the energy optimal route takes a more direct path to its destination in order to preserve energy, whereas the more risk optimal route is more careful to avoid high risk areas and expends more energy doing so.

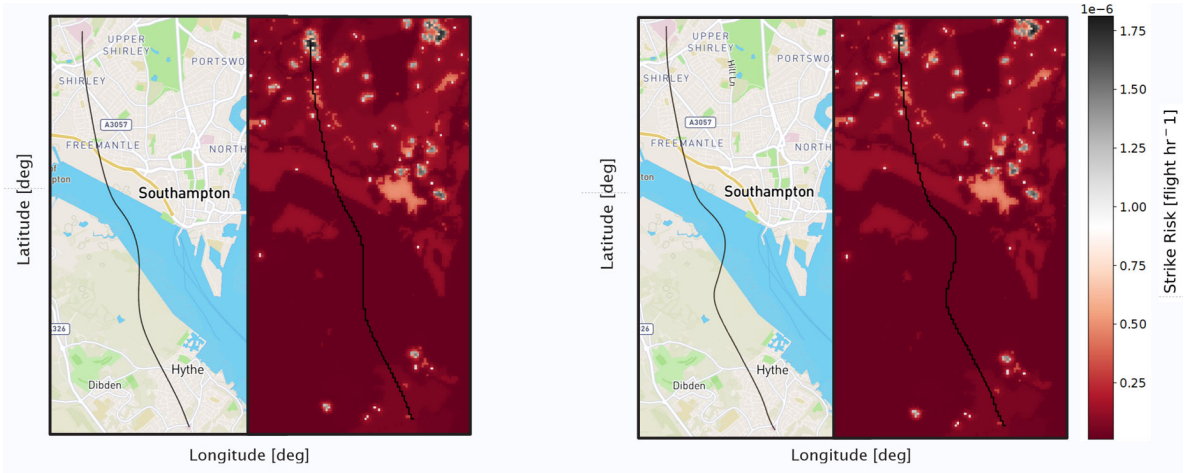

Figure 1: A figure showing how the generated trajectory changes when α is changed from $\alpha = 5 \times 10^8$ (left) for a more energy optimal route to $\alpha = 5 \times 10^9$ (right) for a more risk optimal route.

References

[1] Pierpaolo Murrieri Samir Bouabdallah and Roland Siegwart. Towards autonomous indoor micro vtol. *Autonomous robots*, 18:171–183, 03 2005.

[2] Alexander Blakesley, Bani Anvari, Jakub Krol, and Michael G.H. Bell. Minimum energy route optimisation of a quad-copter uav with landing incentivisation. In *2022 IEEE 25th International Conference on Intelligent Transportation Systems (ITSC)*, pages 2300–2306, 2022.

[3] Dji phantom 2 specifications webpage.

[4] Fabio Morbidi, Roel Cano, David Lara, and et al. Minimum-energy path generation for a quadrotor uav. In *2016 IEEE International Conference on Robotics and Automation (ICRA)*, pages 1492–1498, 2016.

[5] Matthew Kelly. An introduction to trajectory optimization: How to do your own direct collocation. *SIAM Review*, 59(4):849–904, 2017.

[6] Andreas Wächter. On the implementation of an interior-point filter line-search algorithm for large-scale nonlinear programming. *Mathematical Programming*, 106(25):1436–4646, 2006.

[7] Roy Welch and Andrew R. Homsey. Datum shifts for utm coordinates. *Photogrammetric Engineering and Remote Sensing*, 63:371–375, 1997.